Supporting information for: Field-Enhanced Selectivity in Nanoconfined Ionic Transport

Ke Zhou and Zhiping Xu*

Applied Mechanics Laboratory, Department of Engineering Mechanics, Tsinghua University, Beijing 100084, China

E-mail: xuzp@tsinghua.edu.cn

Contents

S1 Supplementary Notes

S1.1 The dissociation of confined bilayer water under an external electric field

First-principles Born-Oppenheimer MD (BOMD) simulations were performed using the CP2K package.[S1] We use a hybrid Gaussian and plane waves (GPW) scheme where the electronic density is expanded in the form of plane waves with a cutoff of 500 Ry.[S2] The molecularly optimized Gaussian basis sets are used.[S3] Revised Perdew-Burke-Ernzerh (revPBE) parametrization is used for the exchange and correlation functional with Grimmes empirical dispersion corrections (D3).[S4–S6] Goedecker-Teter-Hutter pseudopotentials are used to treat the core electrons.[S7] It was shown in previous studies that the combination of revPBE and D3 predict experimentally consistent structural and dynamical properties of bulk water.[S8] The motion of nuclei follows Newtons equations of motion, which is propagated using the velocity Verlet algorithm with a time step of 0.5 fs. The equilibrium is equilibrated in the NVT ensemble using a Nosé-Hoover thermostat.

To study the stability of water molecules in the bulk form (Fig. S9 and S10), we follow the modern theory of polarization and apply periodic EEFs using the Berry-phase method.[S9] The results show that the length of OH bond (l_{OH}) is elongated under EEF with significant fluctuation. Beyond a critical strength of $E_{\mathrm{c}} = 3.0$ V/nm, water dissociation into H_3O^+ and OH^- is observed, and the protons migrate along the H-bond chain via the Grotthuss transfer mechanism,[S10,S11] in consistency with previous Car-Parrinello MD simulation results.[S10]

For nanoconfined bilayer water, we use a slab model (Fig. S9). Non-periodic EEFs are applied by directly adding an external potential to the ionic and electronic Hamiltonian. The graphene wall is modelled by a 9-3 L-J potential, $V = \varepsilon[\frac{2}{15}(\frac{\sigma}{z})^9 - (\frac{\sigma}{z})^3]$, which is imposed on the oxygen atoms. The parameters $\varepsilon = 0.1$ eV and $\sigma = 4.1$ Å are taken from Ref.[S12] We find that the value of l_{OH} is insensitive to the EEF and self-dissociation cannot be identified in our 10 ps-long BOMD simulations (Fig. S11). This result can be explained by the facts

that the dielectric constant[S13] along the z direction for bilayer water is significantly reduced from $\sim$ 80 for bulk water to $\sim$ 2.0, which in turn elevates the free energy barrier of self-dissociation,[S14] and the continuous H-bond network that is necessary for proton migration is broken by the presence of walls. Moreover, the water configurations in nanochannel are modified by the EEF. In the absence of EEF, the distributions of OH bond orientation angle (θ) in water molecules has a peak at 20° (or 160°) and 100° (or 80°) for the bottom (or top) water layer, which is consistent with the MD simulation results using atomistic graphene walls.[S15] The peak in the bottom layer shifts to 90° under EEF, with the OH bond lying in parallel to the surface, and 165°, where the OH bond is almost perpendicular to surface. These two configurations effectively inhibit the elongation of l_{OH} and thus water dissociation because of the reduced electrostatic potential difference across the OH group along the z direction and wall repulsion, respectively.

Previous studies show that the presence of ions in water reduces the threshold EEF for water dissociation from 3.5 to 2.5 V/nm.[S16] To explore this effect under nanoconfinement, we added Na^+ and Cl^- in to both bulk and nanoconfined bilayer water. The results show that for bulk water at $E = 3$ and 4 V/nm, the O–H bonds in water molecules are stretched with the presence of charged ions (Fig. S10), which promotes the dissociation of water molecules by breaking the H-bond network. However, for bilayer water, the distribution of l_{OH} remains almost intact with the addition of ions up to 20 V/nm (Fig. S15), indicating no dissociation of water. The explanation due to the strong confinement effect on the H-bond network still hold for this finding.

S1.2 Additional discussion on the force-field parameterization

We use an alternative set of force-field parameters developed by Williams and co-workers to valid our conclusion reached from the approach introduced in the main text.[S17] The 12-6 L-J parameters between ions and carbon atoms in graphene are fitted from DFT-calculated PMF for an ion near a graphene surface. Our results indicate that the ion trajectories and FEL are similar as those plotted in Figs. 3 and 4a. The SDDF for water and ions, self-diffusion coefficients (D), and selectivity (S) are plotted Fig. S13 as a function of the field strength, E. The value of D is reduced beyond at a critical field strength of $E = \sim 5$ and ~ 10 V/nm for Na^+ and K^+, respectively. The value of S_{K^+/Na^+} increases from less than 2.0 at $E < \sim 5$ V/nm to higher than 30.0 at $E = 20$ V/nm. These results validate our conclusions obtained from the force field developed by Kenneth and co-workers.[S18]

S1.3 Near-surface diffusion of ions in *h*-BN and MoS_2 nanochannels

We study near-surface diffusion of ions in h-BN and MoS_2 nanochannels using force-field parameters summarized in Table S4.[S19,S20] The interlayer spacings are 1.02 and 1.295 nm for the h-BN and MoS_2 channels, respectively, which correspond to an effective channel width or the thickness of water layers of 0.68 nm that is the same as the value considered for the graphene channels. The 12-6 L-J parameters between the ions and atoms in the walls are determined from the Lorentz-Berthelot mixing rules. The FELs of Na^+ in the h-BN and MoS_2 nanochannels are plotted in Fig. S14 for $E = 10$ and 20 V/nm.

S2 Supplementary Tables, Figures and Captions

Table S1: The ion-water PDF measured for Na^+. Here p_1 and v_1 are the positions of the first peak and valley, respectively. g_1 is the height of the first peak, and N_c is the number of water molecules in the 1HS.

E (V/nm)	p_1 (nm)	g_1	v_1 (nm)	N_c
0	0.2325	8.10	0.3155	5.41
5	0.2325	8.16	0.3075	5.35
7.5	0.2325	7.50	0.3025	4.79
10	0.2325	5.75	0.3075	3.92
15	0.2325	4.67	0.3025	3.59
20	0.2375	4.00	0.3125	3.29

Table S2: The self-diffusion coefficients (D) of water and the population of hydrogen bond (n_{HB}) with E ranging from 0 to 20 V/nm. The geometry-based criterion is used to analyze the H-bond network, including the distance between the oxygen of both molecules is smaller than 0.36 nm, the distance between the oxygen of the acceptor and the hydrogen of the donor is smaller than 0.245 nm and the angle defined within the dimer geometry is smaller than 30°.[S21]

E (V/nm)	$D(\times 10^{-9}\mathrm{m}^2/\mathrm{s})$	n_{HB}
0	2.37 ± 0.03	3.27
5	2.61 ± 0.03	3.13
10	3.73 ± 0.01	2.83
15	4.07 ± 0.02	2.64
20	3.75 ± 0.01	2.53

Table S3: The average time interval (Δt) between jumping events from one site to another in the near-surface ion diffusion process.

E (V/nm)	Δt (ps)
0	0.23
5	0.54
7.5	0.64
10	1.27
15	8.03
20	130.42

Table S4: The 12-6 L-J parameters used for h-BN and MoS_2. Here OW denotes the oxygen atom in a water molecule.

	$q(e)$	σ (nm)	ε (kcal/mol)
B	+0.37	0.3309	0.0692
N	-0.37	0.3217	0.0473
B-OW	/	0.3310	0.1214
N-OW	/	0.3266	0.1500
Mo	+0.76	0.4200	0.0135
S	-0.38	0.3130	0.4612
M-OW	/	0.3376	0.2379
S-OW	/	0.3500	0.6779

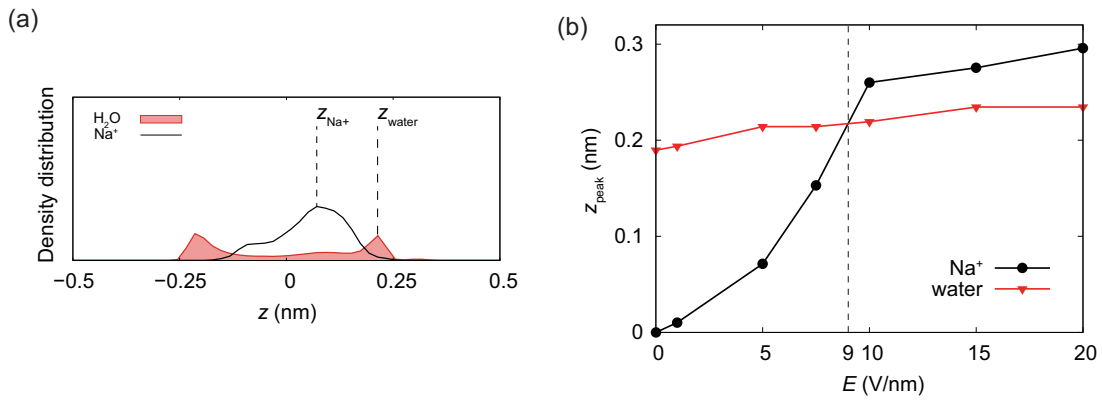

Fig. S1: (a) Density peaks of the Na^+ ion and water in a graphene channel. (b) The position of peaks, z, measured under the EEF (Fig. 1c). For reference, the position of channel wall is $z = \pm 0.51$ nm.

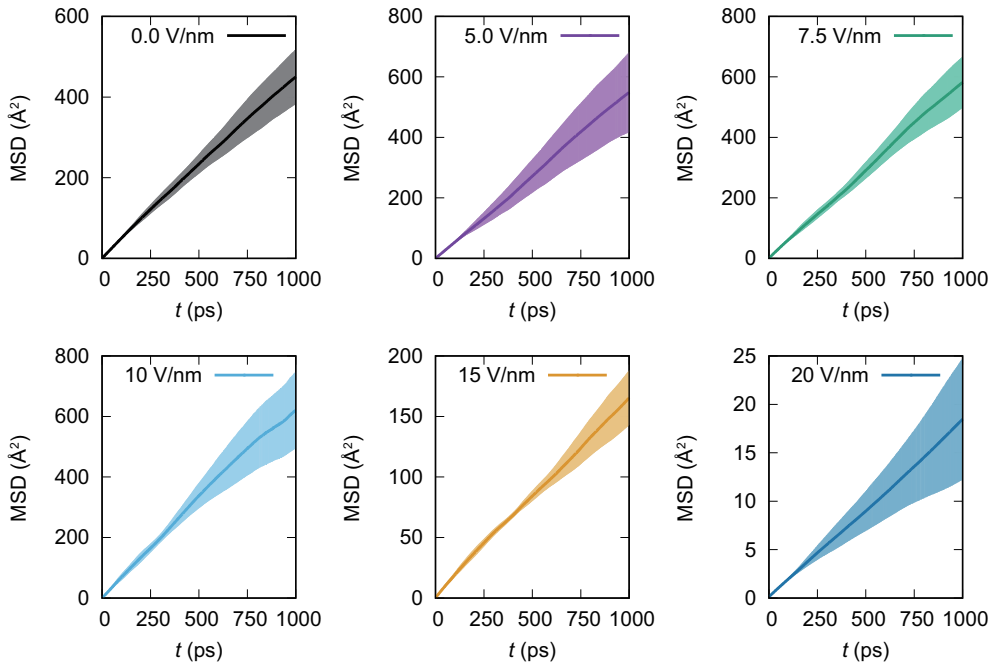

Fig. S2: The MSD curves measured for Na^+ under E = 0-20 V/nm, plotted on normal scales against the time interval. The colored background indicates the range of standard errors. The results plotted on log-log scale are shown in Fig. 1d.

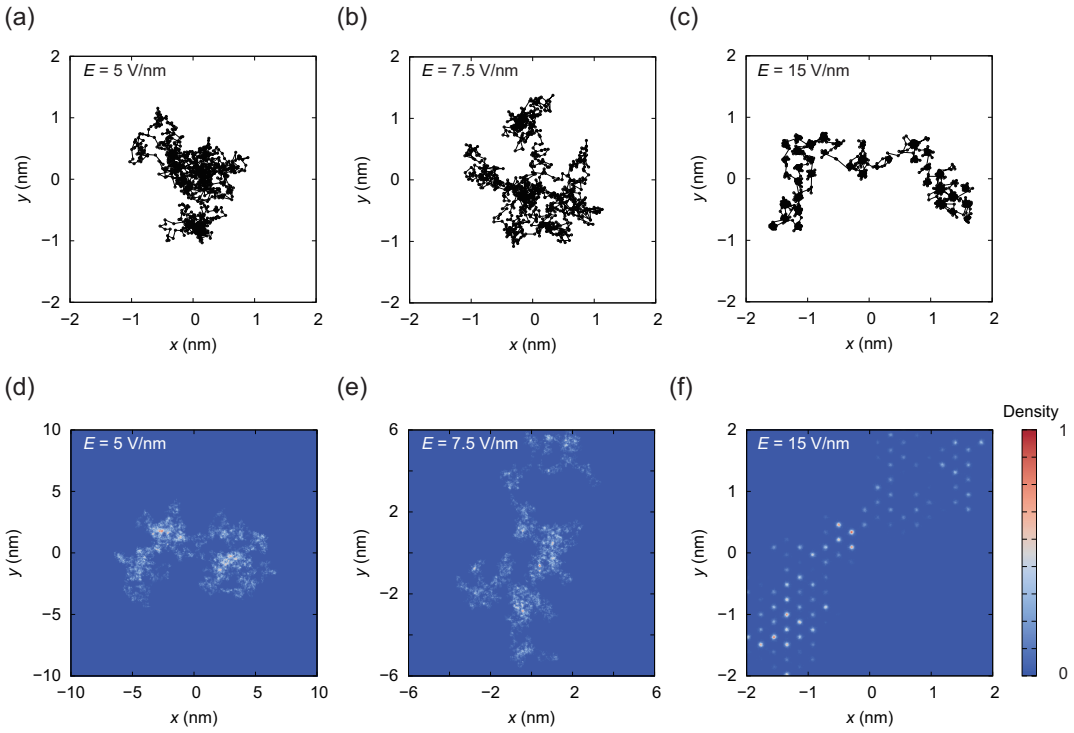

Fig. S3: (a)-(c) Trajectories of Na^+ ions under $E = 5$, 7.5 and 15 V/nm. The time interval is 1 ps. The total time is 1 ns for $E = 0$ and 7.5 V/nm and 2 ns for $E = 15$ V/nm. (d)-(f) The spatial distribution of Na^+ ions. The total time of simulation used to calculate the distribution is 10 ns. The color bar indicates the ion spatial density in the $x - y$ plane.

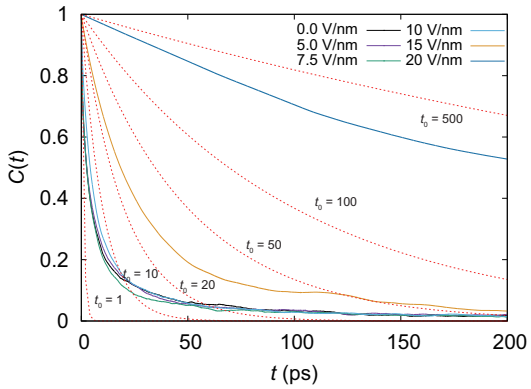

Fig. S4: The self-correlation function used to extract the spatial correlation between ions and site H of the graphene lattice. Here, we estimate the characteristic time t_0 (in unit of ps) for jumping through a single exponential function which is annotated as the red dash line. The results suggest that the value of t_0 is less than ~ 10 ps at $E < 10$ V/nm, and increases significantly at $E > 10$ V/nm.

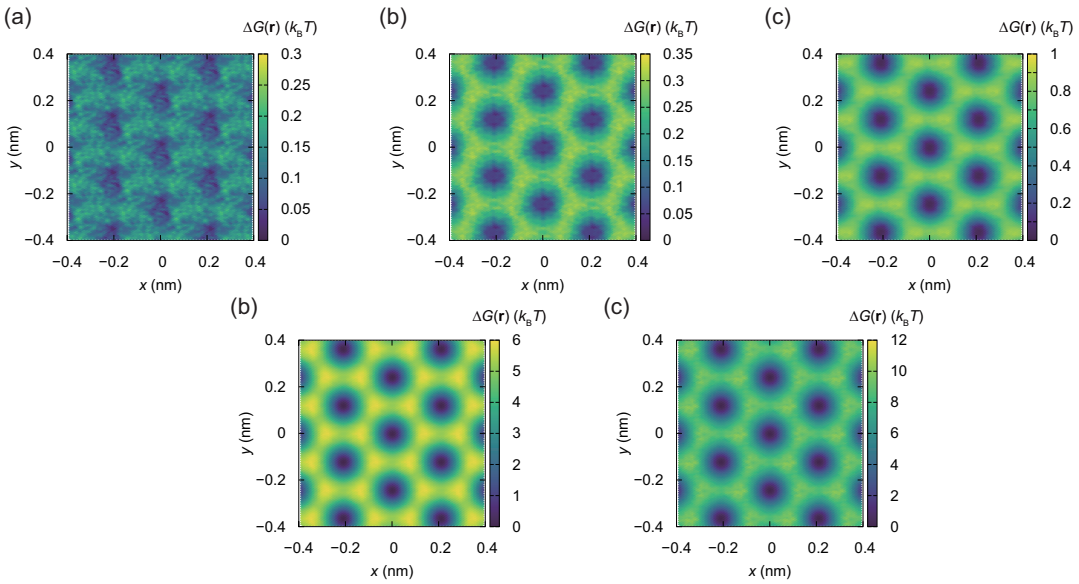

Fig. S5: FELs of Na^+ in a graphene channel measured at (a) $E = 0$, (b) 5, (c) 7.5, (d) 15 and (d) 20 V/nm.

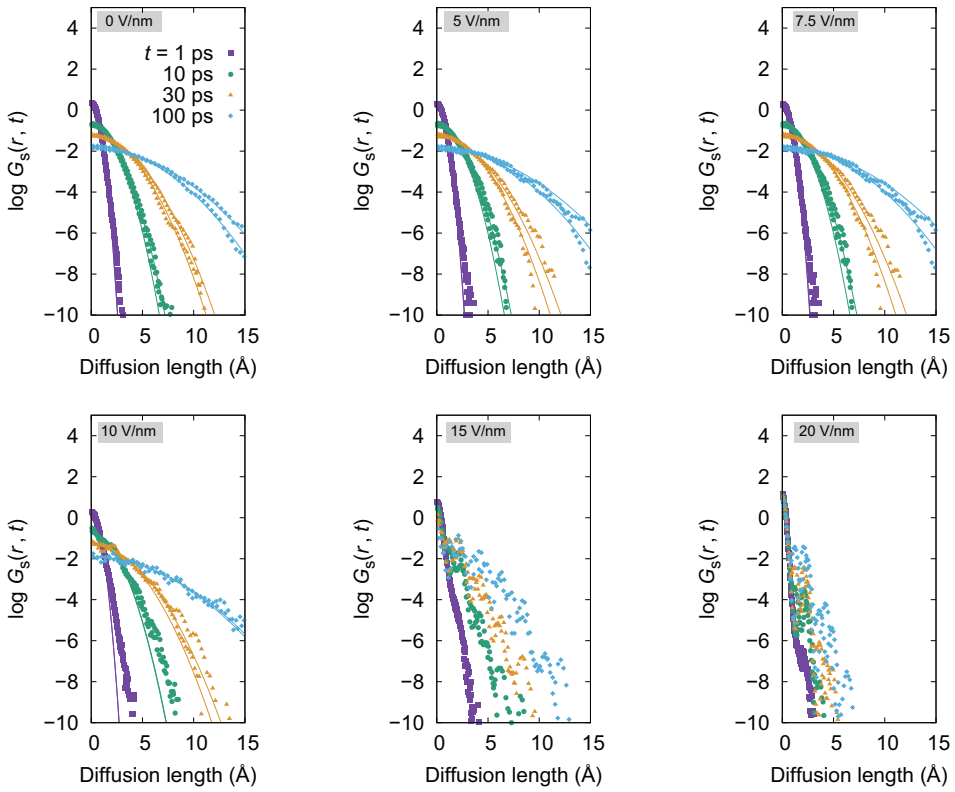

Fig. S6: The self-part of van Hove distribution function $G_{\mathrm{s}}(r,t)$ projected in the x and y directions at $E = 0$ to 20 V/nm. The data in the x or y directions are plotted with the same symbol. The solid lines are the Gaussian fittings.

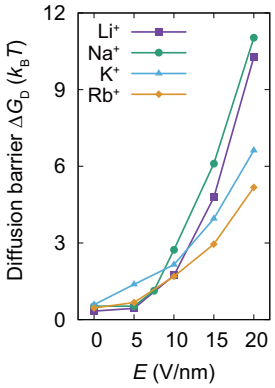

Fig. S7: The diffusion path with the maximal barriers (MBP) of ions in a graphene nanochannel under the EEF. The results for the diffusion path with the minimal barrier (mBP) is shown in Fig. 5b.

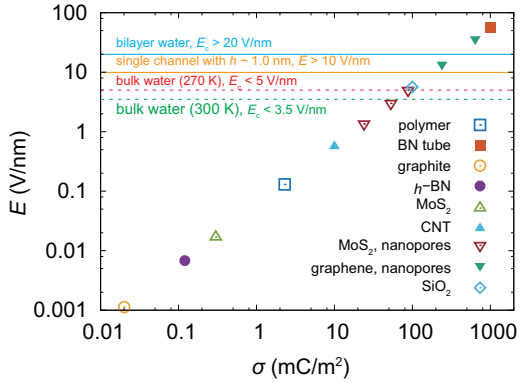

Fig. S8: The strength of local electric fields generated by different surfaces. The references can be found in main text. Several critical strengths are also indicated, including the dissociation strength of bulk water (3.5 V/nm at 300 K and 5.0 V/nm at 270 K), the EEF by applying a voltage of 10 V across a single 1.0 nm-thick channel, and the maximum EEF we applied to the nanoconfined bilayer water where no dissociation was observed.

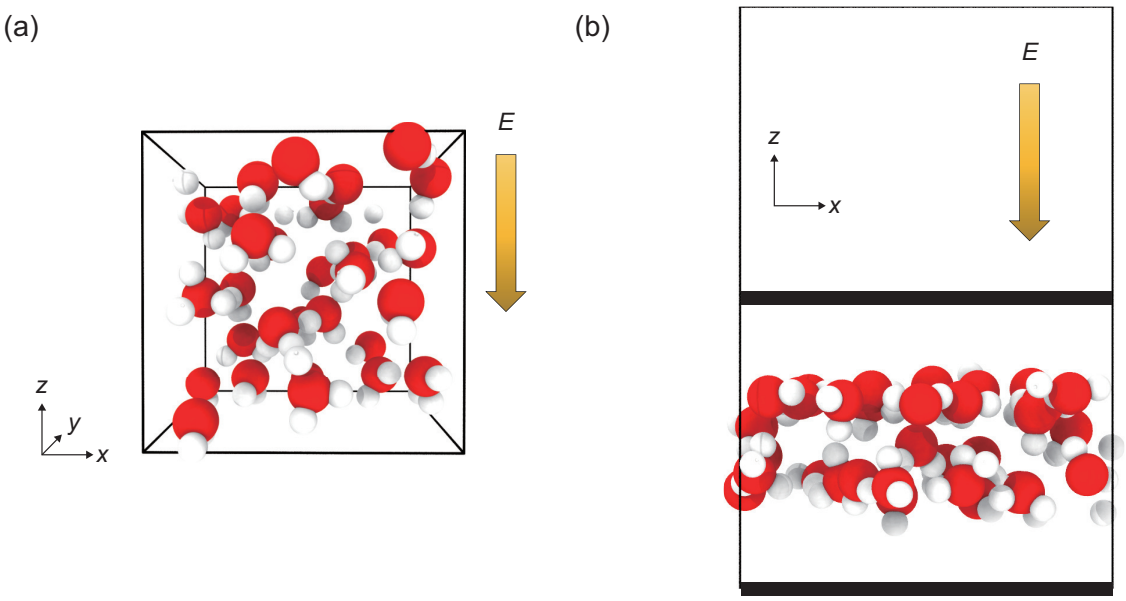

Fig. S9: (a) The simulation box (9.85 × 9.85 × 9.85 Å) containing 32 water molecules for bulk water with a mass density of 1.0 g/cm^3. (b) The simulation box (12.78 × 12.298 × 20.0 Å) containing 32 water molecules for bilayer water confined between two parallel walls (bold black lines) located as $z = 0$ and $z = 10.2$ Å, respectively.

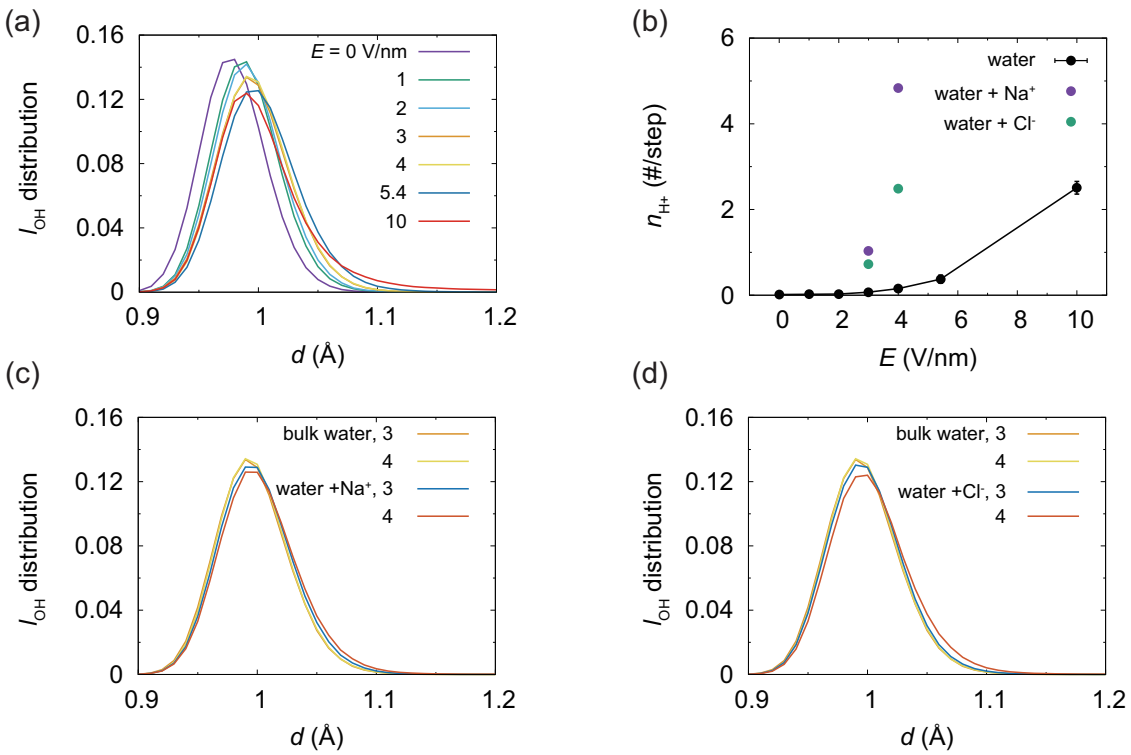

Fig. S10: Structures of bulk water under EEF. (a) Distribution of O–H bond-length (l_{OH}) under EEF ranging from 0 - 10 V/nm. (b) Instantaneous number of protons counted for pure water and water containing Na^+ or Cl^- ions. The ion concentration is 1.74 M. The values plotted for pure water with $E \geq 3$ V/nm are averaged from 2 independent simulation runs. (c)-(d) l_{OH} calculated at $E = 3$ and 4 V/nm for pure water and ion-containing water, showing the elongation of O–H bonds under EEF.

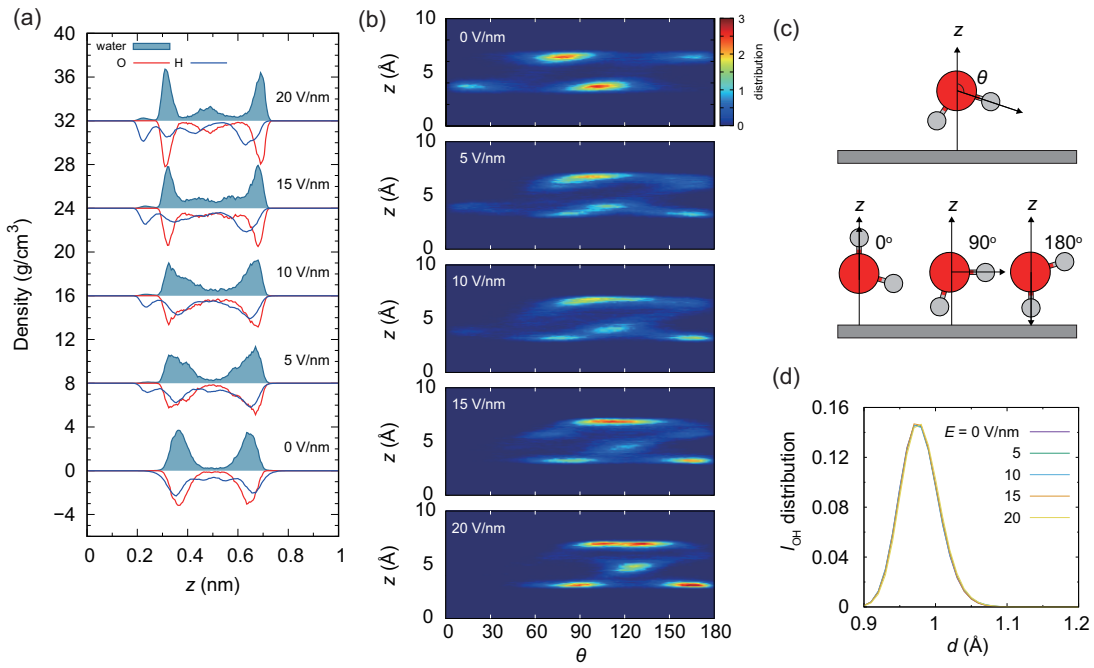

Fig. S11: Structures of nanoconfined water bilayer under EEF. (a) The density distribution of water molecules, and O, H atoms in the z direction. The values for O, H distribution is shown in arbitrary units. (b) Distribution of the OH tilt angle (θ) in water molecules. (c) Typical configurations of water molecules with tilt angles of 0°, 90° and 180°. (d) The bond-length distribution under EEF from 0 - 20 V/nm.

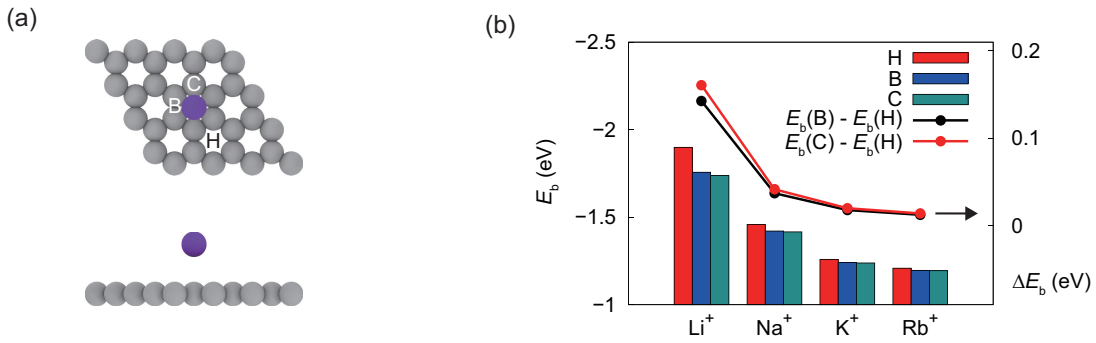

Fig. S12: (a) The supercell model constructed for DFT calculations. The representative sites are highlighted, including the hollow of aromatic ring (`H`), the middle point of C-C bond (bridge, `B`) and the top of C atom (top C, `C`). (b) Binding energies of the alkali ions on the the representative sites, and the diffusion barriers ΔE_{b} calculated as the difference of ΔE_{b} between sites `H` and `B` or `C`.

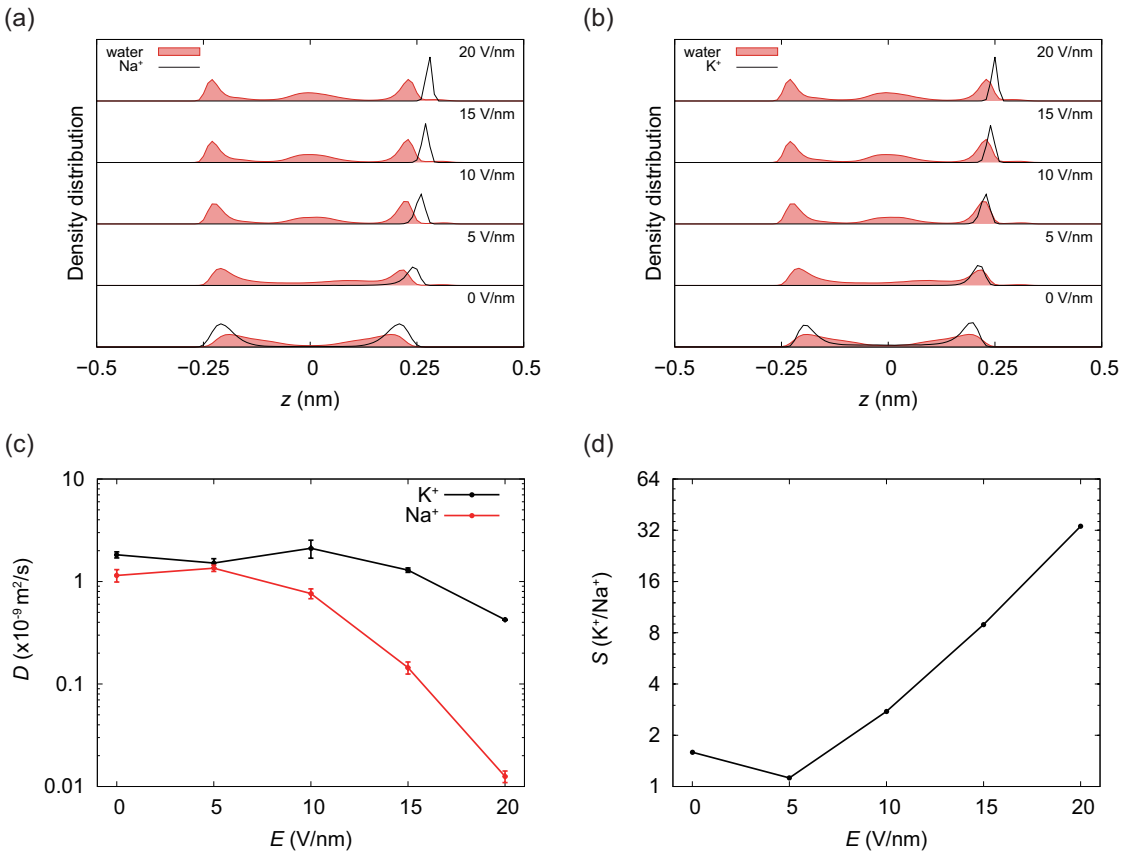

Fig. S13: (a) Self-diffusion coefficients, D, and (b) the selectivity, S, calculated for K^+ and Na^+ ions obtained from MD simulations using force-field parameters provided by Williams and co-workers.[S17]

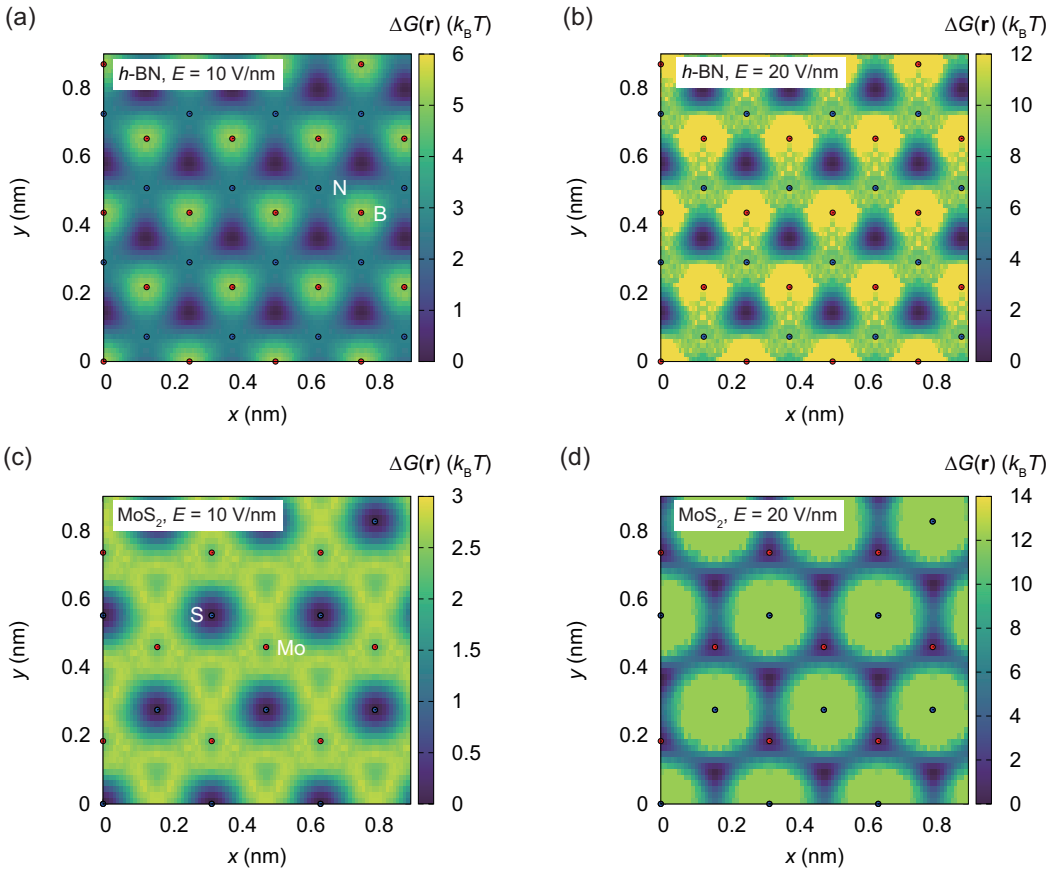

Fig. S14: FELs of Na^+ ions in h-BN and MoS_2 nanochannels with $E = 10$ and 20 V/nm. The positive-charged (B and Mo) and negative-charged (N and S) atoms are colored in blue and red, respectively.

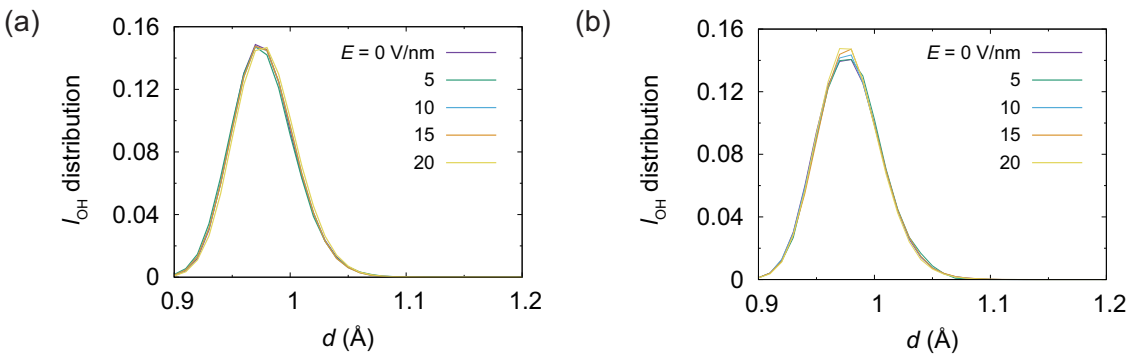

Fig. S15: Distribution of O–H bond-length in nanoconfined water bilayer under EEF ranging from 0 - 20 V/nm, where Na^+ (a) and Cl^- (b) ions are included (1 ion for 32 water molecules).

References

(S1) Hutter, J.; Iannuzzi, M.; Schiffmann, F.; VandeVondele, J. CP2K: Atomistic Simulations of Condensed Matter Systems. *Wiley Interdiscip. Rev.: Comput. Mol. Sci.* **2014**, *4*, 15–25.

(S2) By Gerald, L.; Hutter, J.; Parrinello, M. A Hybrid Gaussian and Plane Wave Density Functional Scheme. *Mol. Phys.* **1997**, *92*, 477–488.

(S3) VandeVondele, J.; Hutter, J. Gaussian Basis Sets for Accurate Calculations on Molecular Systems in Gas and Condensed Phases. *J. Chem. Phys.* **2007**, *127*, 114105.

(S4) Zhang, Y.; Yang, W. Comment on Generalized Gradient Approximation Made Simple. *Phys. Rev. Lett.* **1998**, *80*, 890.

(S5) Perdew, J. P.; Burke, K.; Ernzerhof, M. Generalized Gradient Approximation Made Simple. *Phys. Rev. Lett.* **1996**, *77*, 3865.

(S6) Grimme, S.; Antony, J.; Ehrlich, S.; Krieg, H. A Consistent and Accurate *Ab Initio* Parametrization of Density Functional Dispersion Correction (DFT-D) for the 94 Elements H-Pu. *J. Chem. Phys.* **2010**, *132*, 154104.

(S7) Goedecker, S.; Teter, M.; Hutter, J. Separable Dual-Space Gaussian Pseudopotentials. *Phys. Rev. B* **1996**, *54*, 1703.

(S8) Bankura, A.; Karmakar, A.; Carnevale, V.; Chandra, A.; Klein, M. L. Structure, Dynamics, and Spectral Diffusion of Water from First-Principles Molecular Dynamics. *J. Phys. Chem. C* **2014**, *118*, 29401–29411.

(S9) Umari, P.; Pasquarello, A. *Ab Initio* Molecular Dynamics in a Finite Homogeneous Electric Field. *Phys. Rev. Lett.* **2002**, *89*, 157602.

(S10) Saitta, A. M.; Saija, F.; Giaquinta, P. V. *Ab Initio* Molecular Dynamics Study of Dissociation of Water under an Electric Field. *Phys. Rev. Lett.* **2012**, *108*, 207801.

(S11) Geissler, P. L.; Dellago, C.; Chandler, D.; Hutter, J.; Parrinello, M. Autoionization in Liquid Water. *Science* **2001**, *291*, 2121–2124.

(S12) Zhang, X.; Xu, J.-Y.; Tu, Y.-B.; Sun, K.; Tao, M.-L.; Xiong, Z.-H.; Wu, K.-H.; Wang, J.-Z.; Xue, Q.-K.; Meng, S. Hexagonal Monlayer Ice without Shared Edges. *Phys. Rev. Lett.* **2018**, *121*, 256001.

(S13) Fumagalli, L.; Esfandiar, A.; Fabregas, R.; Hu, S.; Ares, P.; Janardanan, A.; Yang, Q.; Radha, B.; Taniguchi, T.; Watanabe, K.; Gomila, G.; Novoselov, K. S.; Geim, A. K. Anomalously Low Dielectric Constant of Confined Water. *Science* **2018**, *360*, 1339–1342.

(S14) Muñoz-Santiburcio, D.; Marx, D. Nanoconfinement in Slit Pores Enhances Water Self-Dissociation. *Phys. Rev. Lett.* **2017**, *119*, 056002.

(S15) Cicero, G.; Grossman, J. C.; Schwegler, E.; Gygi, F.; Galli, G. Water Confined in Nanotubes and between Graphene Sheets: A First Principle Study. *J. Am. Chem. Soc.* **2008**, *130*, 1871–1878.

(S16) Cassone, G.; Creazzo, F.; Giaquinta, P. V.; Saija, F.; Saitta, A. M. Ab initio molecular dynamics study of an aqueous NaCl solution under an electric field. *Phys. Chem. Chem. Phys.* **2016**, *18*, 23164–23173.

(S17) Williams, C. D.; Dix, J.; Troisi, A.; Carbone, P. Effective Polarization in Pairwise Potentials at the Graphene–Electrolyte Interface. *J. Phys. Chem. Lett.* **2017**, *8*, 703–708.

(S18) Li, P.; Song, L. F.; Merz Jr, K. M. Systematic Parameterization of Monovalent Ions Employing the Nonbonded Model. *J. Chem. Theory Comput.* **2015**, *11*, 1645–1657.

(S19) Wu, Y.; Wagner, L. K.; Aluru, N. R. Hexagonal Boron Nitride and Water Interaction Parameters. *J. Chem. Phys.* **2016**, *144*, 164118.

(S20) Kwac, K.; Kim, I.; Pascal, T. A.; Goddard, W. A.; Park, H. G.; Jung, Y. Multilayer Two-Dimensional Water Structure Confined in MoS_2. *J. Phys. Chem. C* **2017**, *121*, 16021–16028.

(S21) Marti, J.; Padro, J.; Guardia, E. Molecular Dynamics Simulation of Liquid Water along the Coexistence Curve: Hydrogen Bonds and Vibrational Spectra. *J. Chem. Phys.* **1996**, *105*, 639–649.